Correlation between length and tilt of lipid tails

Dmitry I. Kopelevich and John F. Nagle

Citation: The Journal of Chemical Physics **143**, 154702 (2015); doi: 10.1063/1.4932971
View online: http://dx.doi.org/10.1063/1.4932971
View Table of Contents: http://scitation.aip.org/content/aip/journal/jcp/143/15?ver=pdfcov
Published by the AIP Publishing

Correlation between length and tilt of lipid tails

Dmitry I. Kopelevich[1,a)] and John F. Nagle[2,b)]
[1]*Department of Chemical Engineering, University of Florida, Gainesville, Florida 32611, USA*
[2]*Department of Physics, Carnegie Mellon University, Pittsburgh, Pennsylvania 15213, USA*

(Received 1 July 2015; accepted 29 September 2015; published online 16 October 2015)

It is becoming recognized from simulations, and to a lesser extent from experiment, that the classical Helfrich-Canham membrane continuum mechanics model can be fruitfully enriched by the inclusion of molecular tilt, even in the fluid, chain disordered, biologically relevant phase of lipid bilayers. Enriched continuum theories then add a tilt modulus κ_θ to accompany the well recognized bending modulus κ. Different enrichment theories largely agree for many properties, but it has been noticed that there is considerable disagreement in one prediction; one theory postulates that the average length of the hydrocarbon chain tails increases strongly with increasing tilt and another predicts no increase. Our analysis of an all-atom simulation favors the latter theory, but it also shows that the overall tail length decreases slightly with increasing tilt. We show that this deviation from continuum theory can be reconciled by consideration of the average shape of the tails, which is a descriptor not obviously includable in continuum theory. © *2015 AIP Publishing LLC.* [http://dx.doi.org/10.1063/1.4932971]

I. INTRODUCTION

Membranes must undergo extensive shape changes, driven by active energy consuming processes for some biological processes, or by undergoing passive, thermally activated, fluctuations. Either way, it is important that membranes be flexible so as not to incur excessive energies.[1] Such flexibility and elasticity are described by their mechanical properties which are a well recognized part of the study of biomembranes.

On length scales significantly exceeding bilayer thickness, the dominant contribution to the elastic energy of a bilayer is due to bending modes, as described by the classical Helfrich model,[2]

$$F_{\mathrm{H}} = \frac{\kappa}{2}(\nabla \cdot \mathbf{N})^2. \tag{1}$$

Here, the mechanical property of the membrane is the bending modulus κ which scales the free energy F_{H} of a single bilayer leaflet when it undergoes curvature $\nabla \cdot \mathbf{N}$, where $\mathbf{N}$ is the unit normal to the surface. (The Gaussian and spontaneous curvature terms are neglected in Eq. (1) since they do not contribute to the total energy of a symmetric membrane with fixed topology.)

Model (1) neglects contributions of internal degrees of freedom of a bilayer. There are, of course, many internal degrees of freedom associated with molecular conformations, especially in the fluid, so-called liquid-crystalline, phase that are most biologically relevant. It is inappropriate to attempt to incorporate all these into a continuum model that only allows for a description based just on continuous planar coordinates (x, y). Nevertheless, the membrane mechanics field has been moving towards inclusion of a few internal degrees of freedom that describe molecules at a more local level, but still within the continuum framework. A notable early example included molecular tilt in a theory of the ripple phase that occurs at lower temperature.[3] Hamm and Kozlov (HK) presented a tilt-dependent model for the fluid phase,[4,5] which has been substantially reworked by Brown's group.[6] Inclusion of tilt has important implications for estimating the energies required for membrane fusion and inclusion of additives such as membrane proteins.[7,8] Theoretical development combined with simulations[9,10] has definitively shown that either tilt dependent theory accounts for deviations in the Fourier spectrum for larger wavevector q (shorter distances) compared to the tilt independent theory (Eq. (1)). Recently, x-ray scattering experiments[11] have provided the first experimental evidence for tilt in lipid bilayers at the continuum level of molecular mechanics and measured the corresponding material tilt modulus κ_θ.

While the Kozlov[5] and Brown[6] theories agree in many respects, it was recently noticed[12] that the latter theory has a subtly different spectrum when surface tension is applied.[13] This difference was traced to how the length of chains depends on their tilt. The Brown spectrum[13] is consistent with chains maintaining the same average length independent of tilt, as we verify explicitly in this paper. In contrast, tilted chains become longer in the Kozlov theory. This difference leads to different ways to theoretically predict the value of the tilt modulus; the Kozlov way[14] predicts a larger value, $\kappa_\theta \approx 160$ mN/m than the value, $\kappa_\theta \lessapprox 100$ mN/m, if tilted chains maintain the same average length.[12] Interestingly, a third theory, based on the polymer brush model,[15] also predicts $\kappa_\theta \approx 100$ mN/m, but makes a different prediction about the relation between length and tilt than either the Kozlov or Brown theories. The main purpose of this paper to test these predictions using simulations in Section III. We also take this opportunity to further elucidate the relationship of different theories in Section IV. Section V explores a different way to reconcile the remaining minor difference between simulations and theory. First, in Section II the notation and basic theoretical equations are reviewed.

a)Author to whom correspondence should be addressed. Electronic mail: dkopelevich@che.ufl.edu
b)Electronic mail: nagle@cmu.edu

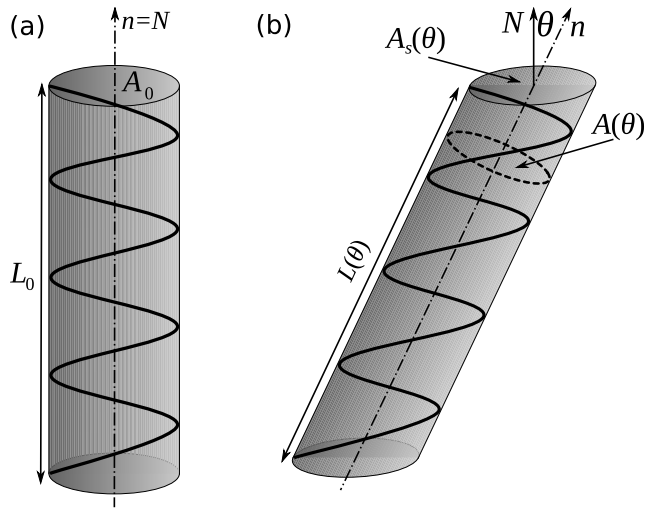

FIG. 1. Schematics of a lipid tail (a) parallel to the monolayer normal and (b) tilted by angle θ with respect to the normal. The notion that a lipid molecule takes on an average cylindrical shape which then wobbles was proposed by Chan and co-workers[16,17] and has been supported by MD simulations.[18]

II. THEORETICAL BACKGROUND

The tilt vector $\mathbf{m}$ is customarily[3,5] defined as

$$\mathbf{m} = \frac{\mathbf{n}}{\mathbf{n}\cdot\mathbf{N}} - \mathbf{N}, \tag{2}$$

where $\mathbf{n}$ is the lipid director of unit length. Throughout this work, vectors $\mathbf{n}$ and $\mathbf{N}$ are oriented so that they point from tail to head, as shown in Fig. 1. The tilt vector characterizes deviation of the lipid director from the monolayer normal; $|\mathbf{m}| = \tan\theta$, where θ is the angle between $\mathbf{n}$ and $\mathbf{N}$.

In the model of HK,[5] free energy of a monolayer, per unit area of its projection, is

$$F_{\mathrm{HK}} = \frac{\kappa}{2}(\nabla\cdot\mathbf{n})^2 + \frac{\kappa_\theta}{2}|\mathbf{m}|^2, \tag{3}$$

where here κ_θ denotes the monolayer tilt modulus. In the absence of lipid tilt, $\mathbf{m} = 0$, $\mathbf{n} = \mathbf{N}$, and the first term of (3) contains the monolayer curvature $C = \nabla\cdot\mathbf{N}$. Hence, in this case (3) reduces to the classical Helfrich model.[2] By analogy with the surface curvature C, the divergence of the tilt director is referred to as the effective curvature $\tilde{C} = \nabla\cdot\mathbf{n}$.

HK model (3) assumes that the dividing surface of the monolayer is incompressible. This implies that a tilted tail is, on average, longer than an untilted one. To see this, approximate a lipid tail by a cylinder of mean length $L(\theta)$ and cross-sectional area $A(\theta)$, as illustrated in Fig. 1. The generally accepted volume incompressibility of the chains, applicable to all models considered in this work, implies that

$$A(\theta)L(\theta) = A_0L_0, \tag{4}$$

where $A_0 = A(0)$ and $L_0 = L(0)$ are the mean values of A and L for untilted chains. The interfacial area of a tilted chain is

$$A_s(\theta) = \frac{A(\theta)}{\cos\theta}. \tag{5}$$

The incompressible surface (IS) assumption of the HK model (3) corresponds to $A_s(\theta) = A_0$. This implies that

$$L^{IS}(\theta) = L_0/\cos\theta, \tag{6}$$

i.e., tilted tails elongate to maintain constant monolayer thickness. The tilt modulus then measures the free energy of chain stretching, and it was estimated[14] that $\kappa_\theta^{IS} \approx 80$ mN/m for monolayers.

A different assumption, namely, that the mean chain length $L(\theta)$ does not vary with chain tilt, has been recently proposed.[12] In this invariant length (IL) model, a tilted lipid tail shown in Fig. 1 would have $L^{IL}(\theta) = L_0$ and $A(\theta) = A_0$, so the chain conformational energy would not necessarily change with chain tilt. The chain area exposed to the interface is $A_s(\theta) = A_0/\cos\theta$, so the hydrophobic energy penalty per unit area associated with a tilted chain is

$$\Delta F = \gamma_{\mathrm{ow}}(A_s(\theta) - A_0)/A_s(\theta) = \gamma_{\mathrm{ow}}(1 - cos\theta) \approx \gamma_{\mathrm{ow}}\mathbf{m}^2/2, \tag{7}$$

where γ_{ow} can be thought of as oil/water surface tension, and we used $|\mathbf{m}| = \tan\theta$ and the small angle approximation. Comparing Eqs. (7) and (3), it was proposed that the leading order contribution to the tilt energy is due to this hydrophobic interaction; this yields $\kappa_\theta^{IL} = \gamma_{\mathrm{ow}} \approx 40$–$50$ mN/m for a monolayer and 80–100 mN/m for a bilayer.

The contribution of the interfacial tension to the tilt modulus is in agreement with the Brown theory,[6] which predicts $\kappa_\theta = \gamma_{\mathrm{ow}} - B/A_0^2$ for a monolayer (see also Section IV C). The additional term B/A_0^2 represents repulsive head-group interactions which were not included in the simple IL model.[12]

This section shows that the dominant contribution to κ_θ can be identified by analysis of the correlation between the chain tilt and length. No correlation would indicate the validity of the IL model with the tilt modulus dominated by the interfacial tension. A positive correlation would indicate that the free energy of chain stretching should be considered. A very strong correlation conforming to Eq. (6) would support the validity of the IS model with the free energy of chain stretching providing the dominant contribution to κ_θ.

III. ANALYSIS OF MD SIMULATIONS

A. Methods

Relationship between the length and tilt of lipid tails was investigated by analysis of MD simulations of dipalmitoyl-phosphatidylcholine (DPPC) and dilauroyl-phosphatidylcholine (DLPC) lipid bilayers. The simulations had been performed by Khelashvili using the CHARMM36 force field[19,20] following the protocol described in Ref. 21. The MD trajectories provided to the authors consisted of full molecular configurations saved every 40 ps. Both systems contained 128 lipid molecules, with DPPC and DLPC bilayers solvated by 4539 and 5034 water molecules, respectively. Temperature, pressure, and the membrane tension were maintained at 50 °C, 1 atm, and 0 mN/m, respectively. Each system was equilibrated for 110 ns followed by a 120 ns production run. Sizes of the equilibrated DPPC and DLPC systems were $6.2\times6.1\times7.6$ nm^3 and $6.3\times6.3\times6.9$ nm^3, respectively, with the bilayers parallel to the x–y plane.

In the current work, we define the tail director as the vector pointing from the terminal carbon atom C_N to the carbon

atom C_1 connected to the glycerol group. This definition is a departure from the earlier work,[6,9,10] where the director terminated at the head-group. The definition chosen in the current work allows us to focus exclusively on hydrocarbon tail groups. Furthermore, in this paper we focus on directors of individual tails, whereas in the earlier work lipid directors were obtained by averaging over both lipid tails. Effects of this averaging are explored in Section I of the supplementary material.[22] In addition, in the supplementary material[22] we consider an alternative definition of the tail director as a principal direction of gyration of a tail. Both director definitions considered in the supplementary material[22] yield qualitatively the same results for the tilt-length correlations as the director $\overrightarrow{C_N C_1}$ considered in text.

Throughout this paper, we refer to the distance between atoms C_1 and C_N as the length L of the director. This convention is different from the earlier work,[5,6,9] where the lipid director $\mathbf{n}$ was normalized to unity. However, normalization of $\mathbf{n}$ does not affect the definition of the tilt $\mathbf{m}$, see Eq. (2).

In addition to the lipid director $\mathbf{n}$, the definition of lipid tilt involves the normal $\mathbf{N}$ to the monolayer surface. In the current work, we characterize the monolayer shape by the surface $z_1^{(\alpha)}(\mathbf{r})$ passing through all C_1 atoms of the αth monolayer ($\alpha = 1, 2$). To compute the tilt $\mathbf{m}$ of a director $\mathbf{n} = \overrightarrow{C_N C_1}$, we use the surface normal $\mathbf{N}$ defined as the normal to $z_1^{(\alpha)}(x, y)$ evaluated at the point (x_1, y_1), where x_1 and y_1 are the coordinates of the atom C_1.

The calculation of the normal to $z_1^{(\alpha)}(\mathbf{r})$ requires a smooth continuous approximation to this surface. To this end, we use the Fourier series with coefficients obtained by a least-squares minimization,

$$\sum_k \left| z_1^{(\alpha,k)} - z_1^{(\alpha)}\left(\mathbf{r}_1^{(\alpha,k)}\right)\right|^2 \to \min . \tag{8}$$

Here, $\mathbf{r}_1^{(\alpha,k)} \equiv (x_1^{(\alpha,k)}, y_1^{(\alpha,k)})$ and $z_1^{(\alpha,k)}$ are the coordinates of the atom C_1 of the kth tail in the αth monolayer; the summation in (8) is performed over all tails belonging to the αth leaflet. The Fourier sum contains three harmonics in each direction, which corresponds to a high wavenumber cut-off value of 3.0 nm^{-1}.

B. Correlation between tail length and tilt

In order to investigate the effect of tail tilt on its length, averages of the tail director length $\bar{L}(m)$ were obtained at various values of tilt m. Dependence of $\bar{L}(m)$ on m shown in Fig. 2 indicates that, for both considered lipids, the tail lengths become slightly shorter as the tilt increases. Since tail shortening is relatively small, in the first approximation the tilt-length correlations can be described by the IL model.

To further explore effects of the chain tilt on its length, in Fig. 3 we plot conditional distributions $P(L|m)$ of the director length L of DPPC tails for different ranges of tilt m. As tilt increases, the distributions become slightly wider and their peak shifts towards smaller L. Behavior of DLPC is qualitatively similar to that of DPPC. Therefore, in the remainder of this paper we focus on analysis of the DPPC lipid bilayer. Additional data on DLPC are provided in the supplementary material.[22]

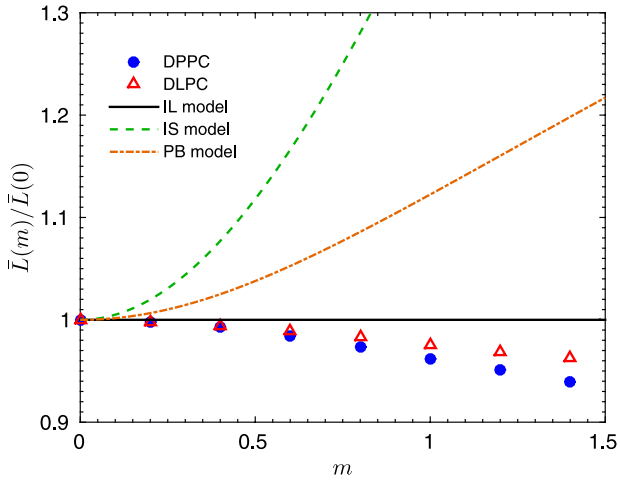

FIG. 2. Dependence of the average tail director length $\bar{L}$ on its tilt m. In this plot, $\bar{L}(m)$ is normalized to its value at zero tilt, $\bar{L}(0) = 1.52$ nm for DPPC and $\bar{L}(0) = 1.11$ nm for DLPC. Standard errors of the plotted $\bar{L}(m)$ are $O(10^{-3})$ nm. For comparison, predictions of the IS, IL, and PB (polymer brush) models are also shown.

IV. ADDITIONAL THEORY

The tilt-induced reduction of the tail length, while small, differs from the assumptions of both models discussed in Sections I and II. In this section we consider more detailed models to explore whether there are other ways to explain this phenomenon as well as to compare theories at a more mathematical level.

A. Polymer brush model

In the polymer brush model,[15] the free energy per chain has both a hydrophobic term proportional to the interfacial chain area A and a chain extension term,

$$F^{PB}(A) = \gamma_{ow} A + \lambda\left(\frac{L}{L_0}\right)^2 = \gamma_{ow} A + \lambda\left(\frac{A_0}{A}\right)^2, \tag{9}$$

where λ is the harmonic energy prefactor and the second equation follows from chain incompressibility (Eq. (4)). The

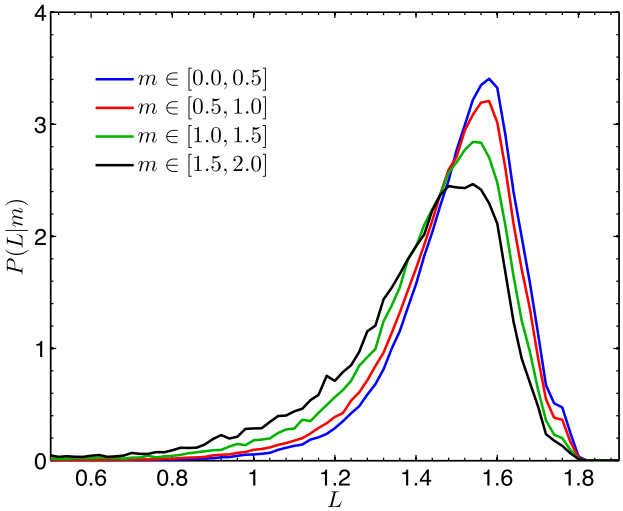

FIG. 3. Conditional probabilities $P(L|m)$ of the director length L of DPPC tails for different ranges of tilt m.

equilibrium chain cross-section area A_0 minimizes $F^{PB}(A)$, thus $\lambda = \gamma_{ow}A_0/2$.

Following a suggestion of Evan Evans, we extend Eq. (9) to a tilted chain,

$$F^{PB}(A,\theta) = \frac{\gamma_{ow}A}{\cos\theta} + \frac{\gamma_{ow}A_0}{2}\left(\frac{A_0}{A}\right)^2. \quad (10)$$

The most probable area $A(\theta)$ for a given tilt θ is obtained by solving $(\partial F/\partial A)_\theta = 0$,

$$\left(\frac{A(\theta)}{A_0}\right)^3 = \cos\theta. \quad (11)$$

Substitution back into Eq. (10) and expansion in powers of θ yields, in the leading order, $\kappa_\theta^{PB} = \gamma_{ow}$ for a monolayer, the same as for the IL model. Combining Eq. (11) with the conservation of chain volume (4), we obtain the most probable chain length,

$$L^{PB}(\theta) = L_0/(\cos\theta)^{1/3}. \quad (12)$$

This prediction is intermediate between the predictions of the two disparate models discussed in Sections I and II. This is not surprising as the polymer brush model combines the hydrophobic interaction that plays the exclusive role in the IL model and the chain conformational energy that plays the exclusive role in the IS model. Interestingly, however, this PB model predicts $\kappa_\theta = 2\gamma_{ow}$ for a bilayer, just like the IL model, even though it includes free energy contributions from both chain extension and area expansion.

B. Opposing forces model

In the polymer brush model in Sec. IV A, the two terms oppose each other in their effect upon the area. A more general opposing forces (OF) model assumes the following free energy per chain:

$$F^{OF}(A_s) = \gamma_{ow}A_s + \frac{B}{A_h} + \tau(L - L_c)^2. \quad (13)$$

The last two terms in Eq. (13) represent interaction between lipid head-groups and the chain stretching, respectively; A_h is the cross-sectional area of the head-group and L_c is the preferred tail length. The polymer brush model is a special case of this OF model corresponding to $B = 0$, $L_c = 0$, and $\tau = \lambda/L_0^2 = \gamma_{ow}A_0/2L_0^2$. This OF model was used by Watson *et al.* (Eq. (11) in Ref. 6) in deriving a continuum model for lipid bilayers (see Subsection IV C). It is straightforward to verify that a simplified version of Eq. (13) with A_h replaced by the chain interfacial area A_s leads to the same continuum model for the bilayer free energy as that obtained in Ref. 6. This replacement affects only the relationships between the elastic moduli of the continuum model and the molecular parameters of the OF model, so we henceforth replace A_h by A_s in Eq. (13).

Using incompressibility of the hydrocarbon chains (Eq. (4)) and extending Eq. (13) to chains tilted by angle θ, we obtain

$$F^{OF}(L,\theta) = \frac{\gamma_{ow}A_0L_0}{L\cos\theta} + \frac{BL\cos\theta}{A_0L_0} + \tau(L - L_c)^2. \quad (14)$$

The most probable chain length L for a given tilt θ is obtained by solving $(\partial F/\partial L)_\theta = 0$,

$$\frac{\gamma_{ow}A_0L_0}{L^2\cos\theta} = \frac{B\cos\theta}{A_0L_0} + 2\tau(L - L_c). \quad (15)$$

It is convenient to define a lengthening coefficient through the relation

$$L(\theta) = L_0(1 + \hat{l}\theta^2/2 + \cdots). \quad (16)$$

Substituting (16) into Eq. (15), the $O(\theta^0)$ and $O(\theta^2)$ terms yield equations for L_0 and $\hat{l}$, respectively,

$$L_0(L_0 - L_c) = \frac{1}{2\tau}\left(\gamma_{ow}A_0 - \frac{B}{A_0}\right), \quad (17)$$

$$\hat{l} = \frac{\gamma_{ow}A_0 + B/A_0}{2(\gamma_{ow}A_0 + \tau L_0^2)} > 0. \quad (18)$$

In particular, in the case of the polymer brush model ($B = 0$, $L_c = 0$, $\tau = \gamma_{ow}A_0/2L_0^2$), Eq. (18) yields $\hat{l} = 1/3$, in agreement with results of Sec. IV A.

To obtain κ_θ, consider the leading order terms of expression (14) for the free energy,

$$F(\theta) \approx \gamma_{ow}A_0 + \frac{B}{A_0} + \tau(L_0 - L_c)^2 + \frac{\theta^2}{2}\left[(\gamma_{ow}A_0 - B/A_0)(1 - \hat{l}) + 2\tau(L_0 - L_c)L_0\hat{l}\right]. \quad (19)$$

Therefore,

$$\kappa_\theta^{OF} = (\gamma_{ow} - B/A_0^2)(1 - \hat{l}) + \frac{2\tau}{A_0}(L_0 - L_c)L_0\hat{l}. \quad (20)$$

In the case of the polymer brush model, this expression simplifies to $\kappa_\theta = \gamma_{ow}$. Also, recall that these results were obtained assuming that $A_h = A_s(\theta)$. If the alternative assumption that A_h is independent of the lipid tilt is made, then Eqs. (17), (18), and (20) are still applicable but now $B = 0$ in these equations.

C. Continuum model

The molecular models in subsections A and B do not account for monolayer curvature. To do so, it is necessary to consider a model that incorporates the basic features of Eq. (3). However, recall that the HK model also assumed incompressibility of the dividing surface of the monolayer. A generalization of Eq. (3) allowing surface compressibility was developed by Watson *et al.*[6,10,13] This model predicts the following free energy of a monolayer per unit area of its projection:[23]

$$F_W(\mathbf{n},\mathbf{m},l) = F_{HK}(\mathbf{n},\mathbf{m}) + \frac{k_A}{2}l^2 + \frac{\Omega}{2}(\nabla\cdot\mathbf{n})l. \quad (21)$$

Here, $l = (L - L_0)/L_0$ is the relative chain stretching, k_A is the areal compressibility modulus, and Ω quantifies the strength of coupling between the lipid length and the effective curvature. Eq. (21) was obtained from OF model (13) by combining it with the following expression:[6]

$$a_s \equiv \frac{A_s - A_0}{A_0} = -l + l^2 + \frac{m^2}{2} - \frac{L_0}{2}\nabla\cdot\mathbf{n} + \frac{L_0^2}{4}(\nabla\cdot\mathbf{n})^2 - \frac{L_0^2}{3}\tilde{K}, \quad (22)$$

where $\tilde{K}$ is the effective Gaussian curvature. Equation (22) includes contributions of the effective curvature neglected in

(4) as well as incompressibility of the chain volume. In the absence of curvature, Eq. (22) is simply a quadratic expansion of Eqs. (4) and (5).

The compressibility modulus k_A contains contributions from the surface tension and the chain stretching terms of OF model (13),

$$k_A = 2\left(\gamma_{\rm ow} + \frac{\tau L_0^2}{A_0}\right). \tag{23}$$

Contribution of the remaining term of (13), the headgroup repulsion, to the surface compressibility vanishes in quadratic approximation (21). On the other hand, the curvature-length coupling strength Ω contains contributions of all three terms of (13).

The derivation of Eq. (21) based on the molecular OF model[6] was substantially different from the original derivation of Eq. (3), which was based on the continuum theory of elasticity.[5] We show in the Appendix that removing the IS assumption from the latter derivation yields the same monolayer free energy (21) as predicted by the OF model.

Since continuum model (21) follows from the OF model, one might expect that the results for the length-tilt correlations obtained for the OF model in Sec. IV B also hold for the continuum model. However, according to Eq. (21), **m** is decoupled from l, since the only term containing **m** in the continuum model is $\kappa_\theta|\mathbf{m}|^2/2$. This discrepancy between the OF and continuum models arises because the tilt-length coupling in OF model (14) is of the 3rd order in small quantities, $O(m^2 l)$, whereas the continuum model is based on the quadratic expansion of the OF free energy. Therefore, in the approximation of the continuum model, m and l are decoupled and the chain lengthening coefficient $\hat{l}$ in Eq. (16) is zero. Expression (20) for the tilt modulus in this case becomes $\kappa_\theta = \gamma_{\rm ow} - B/A_0^2$, in agreement with Ref. 6.

Eq. (21) is a model for free energy of an individual monolayer. However, bilayers are not just two independent back to back monolayers and the interaction between monolayers introduces extra complexity. The bilayer model is considered in the supplementary material.[22] It is shown that the monolayer coupling induces long-range interactions between chain tilt and length. However, within the resolution of the continuum model, the correlation of tilt and length of the same chain is zero.

V. TAIL SHAPE

We have tried unsuccessfully in Sec. IV to account, within the framework of existing theories, for the simulation result shown in Fig. 2, namely, that there is a small decrease in chain length with increasing chain tilt. In this section, we look at our simulation result from the perspective of additional degrees of freedom of the hydrocarbon chain conformations. As is well known, it is the introduction of gauche rotameric disorder that shortens the end to end length of all trans chains. Supposing that the distribution of gauche rotamers is random along chains, it is then likely that the chain shortening with tilt is associated with increased gauche fraction with tilt. This is indeed the case as shown in Fig. 4.

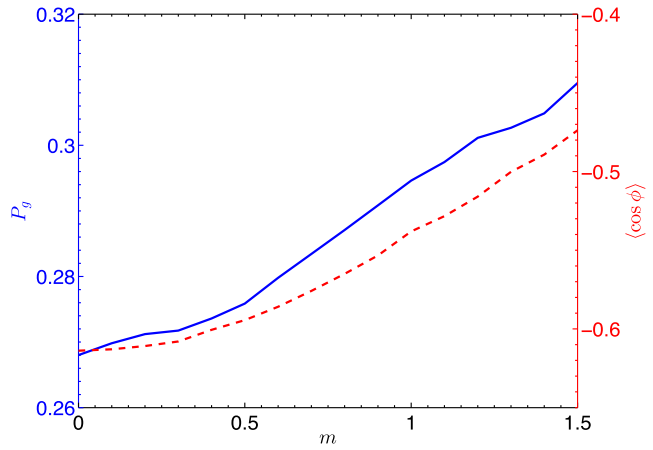

FIG. 4. Fraction P_g of gauche rotamers (solid blue line) and the average relative orientation $\langle\cos\phi\rangle$ (dashed red line) of the directors $\mathbf{n_1}$ and $\mathbf{n_2}$ of the tail segments versus tilt m of the overall tail director **n**.

While tail shortening is qualitatively expected from the result in Fig. 4, we present a simplified analysis that provides both a quantitative estimate of the shortening and additional perspective on the tail shape. Up to this point, we approximated the hydrocarbon chains by cylinders so that the end-to-end distance L has been taken to be the appropriate measure of their length. In this section, we investigate effects of deviations of chains from the cylindrical shape by approximating a lipid tail as two connected cylindrical rods with directors $\mathbf{n_1}$ and $\mathbf{n_2}$, as illustrated in Fig. 5. We define the hinge point as the position of the chain carbon atom C_h located farthest from the chain director. The length of each chain is then approximated as the sum of the lengths, $L_1(m) + L_2(m)$, of the two rods. The difference between the single-rod and two-rod approximation is determined by the angle $\phi = \angle C_1 C_h C_N$ between the directors $\mathbf{n_1}$ and $\mathbf{n_2}$. Fig. 4 shows that, on average, ϕ decreases as the tilt m of the overall tail director **n** increases. This decrease of the mean value of ϕ alone is sufficient to cause the decrease of the overall chain length L if the lengths L_1 and L_2 of the individual segments are independent of m.

Figure 6 shows that the average sum of the lengths of the two rods, $\bar{L}_1(m) + \bar{L}_2(m)$, does indeed decrease much less with increasing m than the overall length $\bar{L}(m)$. The average normalized rod lengths $\bar{L}_1(m)/\bar{L}_1(0)$ (shown in Fig. 6)

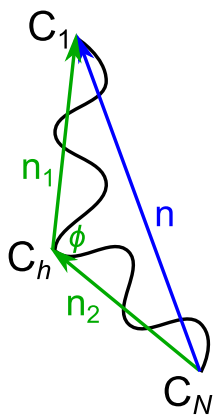

FIG. 5. Approximation of a lipid tail by two connected rods, each with directors $\mathbf{n_1}$ and $\mathbf{n_2}$, meeting at the hinge point C_h.

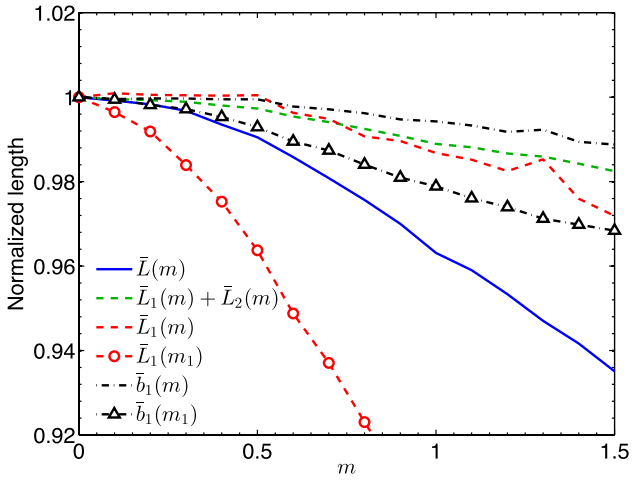

FIG. 6. Comparison of tilt dependence of the mean overall length of tails ($\bar{L}$) with the sum of the two-rod tail segments ($\bar{L}_1$, $\bar{L}_2$), both normalized to the length of tails with minimal tilt. Also compared is the mean length of the first rod as a function of tilt m of the whole chain $\bar{L}_1(m)$ and the same mean length as a function of tilt m_1 of the first rod only $\bar{L}_1(m_1)$, both normalized to their values with minimal tilt. Also compared are the m and m_1 dependences of the mean lengths per methylene group in the first rod $\bar{b}_1 = \langle L_1/h \rangle$. Normalization values were $\bar{L}(m=0) = 1.52$ nm, $\bar{L}_1(m=0) = 0.87$ nm, $\bar{L}_2(m=0) = 0.80$ nm, $\bar{L}_1(m_1=0) = 0.93$ nm, $\bar{b}_1(m=0) = 0.10$ nm, and $\bar{b}_1(m_1=0) = 0.10$ nm.

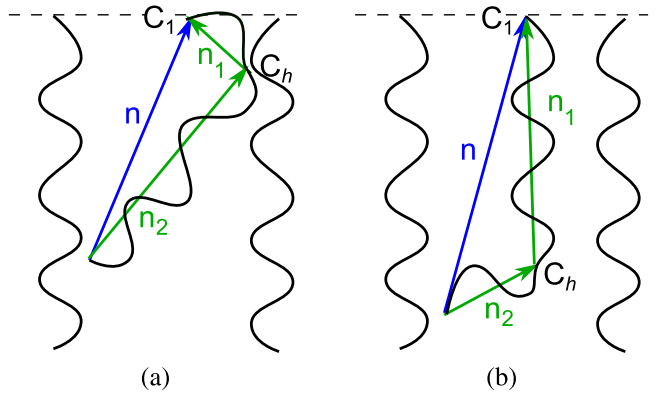

FIG. 7. Schematics of chains with (a) large and (b) small tilt m_1 of the segment C_1-C_h.

and $\bar{L}_2(m)/\bar{L}_2(0)$ (not shown) are also nearly constant with increasing m. Of course, $\bar{L}_1(m)$ and $\bar{L}_2(m)$ decrease with increasing m because the end to end length of each of the rods also underestimates the total length of the individual rod. Indeed, in the limit of decomposing the chain into $N-1$ rods, each consisting of only one carbon-carbon bond, the total length of any chain is the same as an all-trans chain. One could then regard the two-rod approximation as just the first step to approaching this obvious limit. However, the result that this first step takes one so far towards the length being constant with m suggests that it is an appropriate level of description that might also provide insight into chain packing. The utility of the 2-rod model is further supported in Section II C of the supplementary material[22] where it is shown that this model yields a substantially better approximation to the tail shape than a single-rod model, as measured by mean displacements of carbon atoms from relevant directors.

Although the mean rod lengths $\bar{L}_1$ and $\bar{L}_2$ are almost independent of the overall chain tilt m, they are quite sensitive to the tilt m_1 of the chain segment C_1-C_h (m_1 is defined by Eq. (2) with $\mathbf{n}$ replaced by $\mathbf{n_1}$). The dependence of $\bar{L}_1$ on m_1 is shown in Fig. 6. At large m_1, the director $\mathbf{n_1}$ is strongly tilted with respect to the neighboring chains. Therefore, the chain segment C_1-C_h corresponding to this director is likely to experience a steric repulsion from a nearby chain, as illustrated in Fig. 7(a). In this case, h (the number of the hinge atoms C_h in the chain) is likely to be small and, hence, the chain segment corresponding to the director $\mathbf{n_1}$ will be relatively short. On the other hand, at small m_1, the director $\mathbf{n_1}$ is almost parallel to the monolayer normal and steric interactions with neighboring tails are less likely, especially near the headgroup (see Fig. 7(b)). Hence, the hinge point is located nearer the terminal methyl group of the chain and the segment C_1-C_h is relatively longer.

These arguments suggest that the strong dependence of $\bar{L}_1$ on m_1 is caused by the shift of the average location $\bar{h}$ of the hinge carbon atom along the chain rather than shortening of the chain segment C_1-C_h with fixed h. This is supported by the weak dependence on m_1 of the mean length per methylene group of the chain segment, $\bar{b}_1 = \langle L_1/h \rangle$, see Fig. 6. The dependence of $\bar{b}_1$ and $\bar{b}_2$ on the overall chain tilt m is even weaker (see Fig. 6; only $\bar{b}_1$ is shown to avoid cluttering the plot). These observations are consistent with distribution of gauche rotamers along the chains. It is shown in Section II of the supplementary material[22] that the hinge atom C_h is much more likely to belong to a gauche rotamer than atoms in the interior of the segments C_1-C_h and C_h-C_N.

Although in this section we focused on the analysis of a DPPC bilayer, the presented arguments are rather general and are likely to be applicable to a wide range of saturated lipids. This is supported by the tilt-induced tail shortening of DLPC (see Fig. 2). Additional evidence is presented in Section IIA of the supplementary material.[22]

VI. DISCUSSION AND CONCLUSIONS

Our main empirical result is that average chain length decreases as chain tilt increases. This allows us to discriminate between the different theories. Of the three theories shown in Fig. 2, the IL theory clearly agrees best with our simulation results and the IS theory that requires all chains to reach the midplane disagrees most. Surprisingly, the polymer brush theory, being a compromise in the sense that it involves aspects of both the extreme IL and IS theories, disagrees more with the simulations than the IL theory. Even more surprisingly, none of the theories predicts the simulation results that the chain length decreases by a small amount with increasing tilt.

We demonstrated in Section V that the chain shortening can be explained by an effect neglected in the existing models. Specifically, a tilted chain exhibits, on average, larger deviations from the cylindrical shape than an untilted chain and these deviations increase with increasing tilt. We showed that a tilted chain can be adequately approximated by a 2-rod model (see Fig. 5) with mean rod length almost independent of tilt. The decrease of the overall chain length is hence caused by

a decreasing angle between the rods due to steric interactions of a tilted chain with its neighbors (see Fig. 7).

Throughout this paper, we defined a chain director as a vector connecting the chain end-points. It is not inconceivable that the single-rod chain model may still be valid if one chooses a more suitable definition of the chain director that properly accounts for the chain interior. A natural choice for such a director is the principal direction of gyration corresponding to the largest radius of gyration of the chain. Results of analysis performed with this definition of the director are provided in the supplementary material.[22] It is observed that all conclusions obtained with the end-to-end definition of the chain director hold for this alternative definition. In particular, we observe the chain shortening with increasing tilt and a better approximation of the tail shape by the 2-rod model.

The main consequence of the IL assumption, as far as the tilt modulus is concerned, is that the cross-section area of the cylinder approximating the tail chain is independent of tilt. In the 2-rod approximation, it is the cross-section area of the rod connected to the head-group that determines the tilt modulus. This cross-section is constant to a good approximation, since the mean rod length per methylene group, $\bar{b}_1$, is nearly independent of m, see Fig. 6.

It is also likely that the internal degrees of freedom of the 2-rod approximation (i.e., location h of the hinge atom and the angle ϕ between the rod directors) contribute to the tilt modulus. It should be possible to account for these degrees of freedom by performing analysis similar to that in Ref. 14 but without imposing the IS constraint.

Although we know of no model theory which can quantitatively account for the tilt effect on chain shape, it seems appropriate to consider what the existing theories predict for the tilt modulus κ_θ. Both the simple IL and the PB theories predict that κ_θ is twice the surface tension of hydrocarbon and water, namely, $2\gamma_{ow} \approx 100$ mN/m, independent of the lipid. This agrees nicely with the result $\kappa_\theta = 95 \pm 7$ mN/m from a recent x-ray measurement for DOPC.[11] However, unpublished results (Jablin, personal communication) give $\kappa_\theta = 61$ mN/m for DMPC and $\kappa_\theta = 70$ mN/m for SOPC, so it looks like the universality suggested by the simple IL theory may not hold up. Also, simulations are obtaining different values of κ_θ for different lipids. A new review[24] reports 40 mN/m for DMPC and a recent paper[25] gives 64 mN/m for DOPC, both using CHARMM36 and the same analysis methodology.[10] The latter paper also reported 56 mN/m for a united atom simulation of DMPC. In addition to the concern that the simple IL theory prediction that $\kappa_\theta = 100$ mN/m does not allow for lipid variation, it appears that 100 mN/m may be too large. Also, estimates of κ_θ based on NMR or x-ray order parameters[12] are considerably smaller than 100 mN/m. It is therefore important that the more sophisticated IL type theory of the Brown group[6] includes a negative correction term attributed to headgroup repulsion. The magnitude of this negative correction is inversely proportional to the square of the lipid area, thereby predicting a smaller value of κ_θ for DMPC ($A_0 \approx 0.6$ nm^2) than for DOPC ($A_0 \approx 0.7$ nm^2), qualitatively consistent with existing estimates.

The IS theory predicts a larger $\kappa_\theta = 160$ mN/m using a generic mean field calculation.[14] It would, in principle, allow different values of κ_θ for different lipids. However, its dramatic failure revealed in Fig. 2 requires reconsideration. It is intuitively attractive in that bilayer thickness is obviously maintained chain by chain. In contrast, the IL model would appear to violate this intuitive notion that, by having to fill space, chains have to extend from the headgroup to the center of the bilayer. However, this simplistic picture ignores the many conformational degrees of freedom available to chains in their fluid, liquid-crystalline phase. Even without tilt, one can envision a simplistic model with two spatially co-mingled populations of chains. One population would have much conformational disorder so they are short, not extending to the midplane, while the other population would have no conformational disorder at their beginning and much conformational disorder near their ends to fill in the space beneath the chains in the other population that have terminated short of the midplane. Other complications that could be included in other examples are mini-interdigitation with chains extending across the midplane, and upturns with chains moving back to the interface. As simulation snapshots show, the fluid phase is a complex jumble as indicated by the short range of the correlations between tilt of neighboring molecules.[26] This picture is consistent with the difficulty of using intuitive notions of chain packing to predict chain length as a function of tilt, and by extension, the best form of continuum theory of membrane mechanics. Our analysis of simulations overcomes this difficulty.

ACKNOWLEDGMENTS

The authors are grateful to G. Khelashvili for providing trajectories of his MD simulations of DPPC and DLPC bilayers.

APPENDIX: GENERALIZATION OF THE HK MODEL TO INCLUDE SURFACE COMPRESSIBILITY

The purpose of this appendix is to generalize the HK derivation[5] of the monolayer free energy to a monolayer with compressible dividing surface. The starting point of the HK derivation is a quadratic expansion of the elastic energy in terms of the strain tensor. After accounting for symmetry, the free energy of the monolayer per unit volume can be written as[27]

$$f_V(\mathbf{r},\zeta) = \sigma_L a_c + \frac{\lambda_L}{2} a_c^2 + \frac{\lambda_T}{2} m^2. \tag{A1}$$

Here, $\mathbf{r} = (x, y)$, ζ is the distance from the dividing surface along the normal to the monolayer surface, $\sigma_L(\zeta)$ is the lateral stress profile, $\lambda_L(\zeta)$ and $\lambda_T(\zeta)$ are position-dependent elastic moduli, $a_c(\mathbf{r},\zeta) = (A_c(\mathbf{r},\zeta) - A_0)/A_0$ is the relative lateral expansion, A_0 is the area element of an unperturbed monolayer, and $A_c(\mathbf{r},\zeta)$ is the area of a cross-section of the volume element by a surface $\zeta = const$ parallel to the dividing surface of the monolayer. Note that $A_c(\mathbf{r},0) = A_s(\mathbf{r})$, where A_s is the surface area element (see Fig. 1).

HK model (3) can be obtained from Eq. (A1) by expressing a_c in terms of the effective curvature $\nabla \cdot \mathbf{n}$ and integrating f_V over the monolayer thickness. The IS assumption is invoked only to obtain the relationship between a_c and the effective

curvature; Eq. (A1) remains valid for compressible monolayer surfaces.

Let us obtain an expression for a_c applicable to compressible surfaces. To this end, we start with the relationship[5,28] between cross-section area element A_c and the surface area element A_s,

$$A_c(\mathbf{r},\zeta) = A_s(\mathbf{r})(1 + \zeta\nabla\cdot\mathbf{n}(\mathbf{r}) + \zeta^2\tilde{K}(\mathbf{r})). \quad \text{(A2)}$$

Here, $\tilde{K} = \det(\partial n_i/\partial r_j)$ is the effective Gaussian curvature. Therefore,

$$a_c = \zeta\nabla\cdot\mathbf{n} + \zeta^2\tilde{K} + a_s(1 + \zeta\nabla\cdot\mathbf{n}), \quad \text{(A3)}$$

where $a_s(\mathbf{r}) \equiv a_c(\mathbf{r},\zeta = 0)$ is the relative expansion of the surface element. If the IS assumption holds, $a_s(\mathbf{r}) = 0$ and Eq. (A3) reduces to Eq. (25) of Ref. 5.

Substitution of more general expression (A3) into Eq. (A1) yields the following additional terms that are not present in the HK model:

$$a_c \to a_s(1 + \zeta\nabla\cdot\mathbf{n}), \quad \text{(A4)}$$

$$a_c^2 \to a_s^2 + 2\zeta(\nabla\cdot\mathbf{n})a_s. \quad \text{(A5)}$$

The linear in a_s term in (A4) leads to a new term $\sigma_L(\zeta)a_s$ in (A1). Integration of the lateral stress profile $\sigma_L(\zeta)$ over thickness of a tensionless monolayer yields zero, i.e., the linear in a_s term does not contribute to the monolayer free energy. The $a_s\nabla\cdot\mathbf{n}$ and a_s^2 terms in Eqs. (A4) and (A5) combined with Eq. (22) yield the two terms ($l(\nabla\cdot\mathbf{n})$ and l^2) of model (21) of Watson *et al.*[6] that are absent in HK model (3).

[1]J. F. Nagle, Faraday Discuss. **161**, 11 (2013).
[2]W. Helfrich, Z. Naturforsch., C **28**, 693 (1973).
[3]T. C. Lubensky and F. C. MacKintosh, Phys. Rev. Lett. **71**, 1565 (1993).
[4]M. Hamm and M. M. Kozlov, Eur. Phys. J. B **6**, 519 (1998).
[5]M. Hamm and M. M. Kozlov, Eur. Phys. J. E **3**, 323 (2000).
[6]M. C. Watson, E. S. Penev, P. M. Welch, and F. L. H. Brown, J. Chem. Phys. **135**, 244701 (2011).
[7]L. V. Chernomordik and M. M. Kozlov, Annu. Rev. Biochem. **72**, 175 (2003).
[8]L. V. Chernomordik and M. M. Kozlov, Cell **123**, 375 (2005).
[9]E. R. May, A. Narang, and D. I. Kopelevich, Phys. Rev. E **76**, 021913 (2007).
[10]M. C. Watson, E. G. Brandt, P. M. Welch, and F. L. H. Brown, Phys. Rev. Lett. **109**, 028102 (2012).
[11]M. S. Jablin, K. Akabori, and J. F. Nagle, Phys. Rev. Lett. **113**, 248102 (2014).
[12]J. F. Nagle, M. S. Jablin, S. Tristram-Nagle, and K. Akabori, Chem. Phys. Lipids **185**, 3 (2015).
[13]M. C. Watson, A. Morriss-Andrews, P. M. Welch, and F. L. H. Brown, J. Chem. Phys. **139**, 084706 (2013).
[14]S. May, Y. Kozlovsky, A. Ben-Shaul, and M. M. Kozlov, Eur. Phys. J. E **14**, 299 (2004).
[15]W. Rawicz, K. C. Olbrich, T. McIntosh, D. Needham, and E. Evans, Biophys. J. **79**, 328 (2000).
[16]N. O. Petersen and S. I. Chan, Biochemistry **16**, 2657 (1977).
[17]D. F. Bocian and S. I. Chan, Annu. Rev. Phys. Chem. **29**, 307 (1978).
[18]R. W. Pastor, R. M. Venable, and S. E. Feller, Acc. Chem. Res. **35**, 438 (2002).
[19]J. B. Klauda, R. M. Venable, J. A. Freites, J. W. O'Connor, D. J. Tobias, C. Mondragon-Ramirez, I. Vorobyov, A. D. MacKerell, and R. W. Pastor, J. Phys. Chem. B **114**, 7830 (2010).
[20]R. W. Pastor and A. D. MacKerell, J. Phys. Chem. Lett. **2**, 1526 (2011).
[21]G. Khelashvili, B. Kollmitzer, P. Heftberger, G. Pabst, and D. Harries, J. Chem. Theory Comput. **9**, 3866 (2013).
[22]See supplementary material at http://dx.doi.org/10.1063/1.4932971 for (i) analysis with alternative director definitions, (ii) additional analysis of the 2-rod model, and (iii) additional analysis of the continuum model.
[23]In Eq. (21) we neglected the lipid twist energy contained in the model of Watson *et al.*,[6] since this energy is relatively small for bilayers in the fluid phase.[5] Moreover, the twist energy is decoupled from other terms in Eq. (21), see Ref. 6.
[24]R. M. Venable, F. L. H. Brown, and R. W. Pastor, "Mechanical properties of lipid bilayers from molecular dynamics simulation," Chem. Phys. Lipids (in press).
[25]Z. A. Levine, R. M. Venable, M. C. Watson, M. G. Lerner, J.-E. Shea, R. W. Pastor, and F. L. H. Brown, J. Am. Chem. Soc. **136**, 13582 (2014).
[26]G. Khelashvili and D. Harries, J. Phys. Chem. B **117**, 2411 (2013).
[27]Eq. (A1) follows from Eq. (11) of Ref. 5 after neglecting the lateral shear term and substitution of the expression for the tilt term (Eq. (15) of Ref. 5).
[28]Note the sign difference in the definition of the effective total curvature, $\nabla\cdot\mathbf{n}$, employed in the current work and that in Ref. 5.